

Optimal Configurations for Nanosatellite Formation Flying in Binary Asteroid Environment

By Andrea CAPANNOLO,¹⁾ Michèle LAVAGNA,¹⁾ Fabio FERRARI,¹⁾ and Paolo LUNGHI¹⁾

¹⁾*Department of Aerospace Sciences and Technologies, Politecnico di Milano, Milan, Italy*

The exploration of NEA (Near Earth Asteroids) is characterized by many problematics such as collision risks, irregular gravity fields and, in case of binary systems, multibody gravity perturbations, whose negative effects on mission design could be mitigated by the exploitation of multiple spacecraft in formation, with lower weights, dimensions and costs. Nanosatellite fully meet these needs, however, the poor control capabilities, and the strict requirements on relative dynamics to ensure the same performances of a single heavy spacecraft, request an efficient strategy to determine the suitable trajectories in this chaotic environment. The paper proposes a simple technique, based on orbit sampling and local optimization, to define a set of suitable configurations for a two-nanosatellite formation. After a quick review on the orbits determination and combination in binary asteroid environments, and the presentation of the objectives derived from the conceptual mission AIM (Asteroid Impact Mission), the local optimization algorithm is explained, paying attention to the selection of the method and its modification to best adapt to the specific problem. Then, results are presented, showing the strength and weakness points of the overall procedure, for the definition of future improvements.

Key Words: Formation Flying, Binary Systems, Asteroids, Nanosatellite, Optimization

Nomenclature

$CR3BP$: Circular restricted three-body problem
$MCR3BP$: Modified CR3BP
$L1$: Lagrangian point 1
$L2$: Lagrangian point 2
$L4$: Lagrangian point 4
DRO	: Distant retrograde orbits
$HNL1$: Northern Halo orbit around L1
$HSL1$: Southern Halo orbit around L1
$HSL2$: Southern Halo orbit around L2
$\hat{a}, \hat{b}, \hat{c}$: Ellipsoid semi-axes
c	: Constraint equations vector
F	: Objective functions vector
g	: Dynamics equations vector
J	: Cost
J_c	: Overall constrained cost function
J_M	: Jacobian matrix
N	: Number of nodes
N_c	: Number of active constraints
R	: Maximum radius of primary asteroid
r	: Residual of the objective functions
T	: Formation period
X	: State vector of all nodes
x, y, z	: Position coordinates
$\dot{x}, \dot{y}, \dot{z}$: Velocity coordinates
η	: State vector of single node
λ	: Lagrange multipliers

λ_r : Numerical damping parameter

Subscripts

1	: First satellite
2	: Second satellite
p	: Generic projected point
$p1$: First projected point
$p2$: Second projected point
$path$: Trajectory length
prj	: Trajectory projection
rel	: Relative motion

1. Introduction

The optimization of a formation flying configuration, in a chaotic environment such as binary systems, hides its complexity in the presence of very small regions in the state space where periodicity of the solution can be found. The definition of the orbits in this environment, require specific techniques of “correction and continuation”, based on numerical approaches and evaluation of state’s eigenvalues.¹⁾

The presence of irregular gravity fields further aggravates the mentioned drawbacks, removing symmetry properties with respect to the planes of the system. Furthermore, to correctly represent the asteroid’s environment, specific modeling techniques are required, with a consequent increment in the equations complexity, and in the computational costs and time.²⁾

The most straightforward way to overcome these problems is characterized by the exploitation of targeted strategies, where some pre-existent knowledge is used to reduce the solutions

search region. This can be obtained through a hybridization of search methods, exploiting first a sampling based on background knowledge of periodic orbits in these systems, then adopting continuous local optimization algorithms to find the final solution.

Background knowledge of periodic orbits is available when dealing with point mass approximations, in the CR3BP frame, but does not consider the presence of irregular gravity fields. The issue is resolved by a sampling of orbits in the CR3BP, and the subsequent correction into the new gravitational environment through a Newton based multiple shooting scheme. The families of orbits in the asteroid environment are combined to generate a group of suitable configurations, and to select among them the best ones from the evaluation of an overall cost function (derived from mission objectives).

The limitation of this approach lies in the discretization of the search space, which generally leads to sub-optimal solutions. On the other hand, the discretization provides a wide set that can be used as guesses for local optimization process. The advantage of this strategy is due also to the exploitation of the same cost function, that can be directly implemented in the process. The local optimization can be based on a variety of different techniques. In the present work, the Levenberg-Marquardt algorithm has proved to be a very suitable algorithm, since it represents a trade-off between stability (from steepest-descent method) and rate of convergence (from Newton method), provided that the initial guess is sufficiently close to the final solution. Few modifications in the algorithm are applied, to best suit to the intrinsic complexity of the specific problem discussed in the paper, and to enhance the effectiveness of the optimization process. Analytical Jacobian matrix has been computed to significantly speed up the algorithm, from the mathematical computation of derivatives of the single objectives from the cost function.

The results of the optimization are presented and critically discussed, to underline the benefits of the aforementioned approach and propose improvements to overcome the detected drawbacks and issues.

2. Process description

2.1. Objectives definition and model assumptions

In the present work, target objects and objectives from Asteroid Impact Mission concept are considered. The study is limited to a formation of two nanosatellites, in free-dynamics and strictly periodic, non-proximity trajectories.

The asteroid binary system “65803 Didymos” is modeled as follows:

- Main asteroid (“Didymain”) built through polyhedral shaping techniques,³⁾ from real shape observations data.
- Secondary asteroid (“Didymoon”) built as a triaxial ellipsoid,⁴⁾ (in absence of precise shape measurements).

- Revolution period of Didymoon around Didymain of ~12 hours, according to observation.
- Tidal locking of Didymoon with respect to Didymain.
- Rotation period of Didymain assumed equal to revolution period (time invariant binary system in the synodic frame).

Figure 1 shows the appearance of the binary system model.

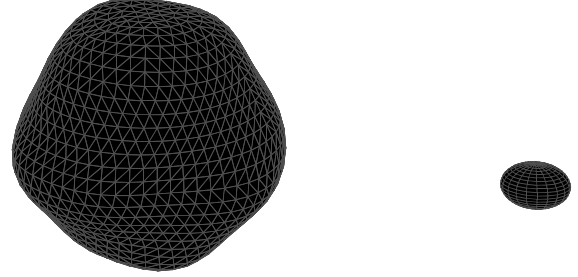


Fig. 1. 65803 Didymos binary system. Didymain (on the left) is modeled as a polyhedral object, while Didymoon (on the right) is represented as an ellipsoid.

The mission objectives considered for the optimization are:

- Relative motion minimization (formation shape maintenance).
- Orbits dimension maximization (gravimetric measurements).
- Maximization of motion around Didymoon (mapping of the internal structure).

The objectives are expressed in dynamic terms to be evaluated by the algorithm. Relative displacement of the satellites is implemented as the integral of squared relative velocity modulus, so that approaching and departure motions are equally reduced.

$$J_{rel} = \int_0^T [(\dot{x}_2 - \dot{x}_1)^2 + (\dot{y}_2 - \dot{y}_1)^2 + (\dot{z}_2 - \dot{z}_1)^2] dt \quad (1)$$

Orbits’ dimension is maximized through the extension of the trajectory within the formation period, expressed as the integral of squared velocity modulus of both spacecraft.

$$J_{path} = - \int_0^T [(\dot{x}_1 + \dot{y}_1 + \dot{z}_1)^2 + (\dot{x}_2 + \dot{y}_2 + \dot{z}_2)^2] dt \quad (2)$$

The motion around Didymoon can be measured in geometrical terms. At each time step, the segment connecting the two spacecraft is traced, and possible intersection with the ellipsoid is searched. In case intersection is present, the two projection points on asteroid’s surface are evaluated in position, velocity and acceleration, according to analytical formulas derived from the equations of tridimensional straight line and triaxial ellipsoid.

With reference to Fig. 2, the system reads:

$$\begin{cases} \sqrt{\left(\frac{x_p + \mu - 1}{a}\right)^2 + \left(\frac{y_p}{b}\right)^2 + \left(\frac{z_p}{c}\right)^2} = 1 \\ y_p = \left(\frac{y_2 - y_1}{x_2 - x_1}\right)(x_p - x_1) + y_1 \\ z_p = \left(\frac{z_2 - z_1}{x_2 - x_1}\right)(x_p - x_1) + z_1 \end{cases} \quad (3)$$

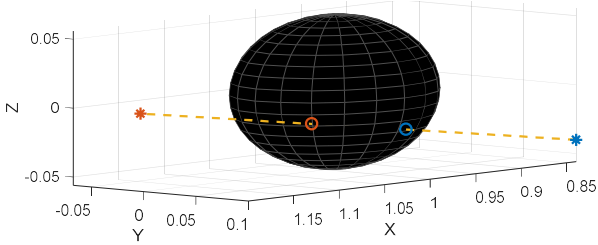


Fig. 2. Representation of the satellites projections on asteroid's surface.

The two solutions derived from Eq. (3) are then included in the cost function in terms of integral of the squared mean velocity norm between the two intersection points.

$$J_{prj} = -\int_0^T \frac{1}{4} \left[(\dot{x}_{p1} + \dot{x}_{p2})^2 + (\dot{y}_{p1} + \dot{y}_{p2})^2 + (\dot{z}_{p1} + \dot{z}_{p2})^2 \right] dt \quad (4)$$

2.2. Guess definition and optimization

To initialize the optimization, a set of possible initial guesses, based on the background knowledge of the problem, is built. It is known how irregular shape objects affect the geometrical properties of trajectories, especially if dealing with binary systems, therefore already known solutions are recovered from the simpler point masses model, in the CR3BP frame. A further step is introduced to move from the point mass model to the asteroids model: gradual shape modification process allows to transform point masses (or spheres) into the real shape of considered objects, while correcting the orbits to fit the new gravitational field,⁵ as shown in Figs. 3 and 4.

The full set of orbits in the asteroids environment is exploited in a preliminary combinatorial optimization. The single dynamical objectives described in Eq. (1), (2) and (4) are combined to form an overall cost function (multi-objective scalarization), as expressed in Eq. (5).

$$J = J_{rel} + J_{path} + J_{prj} \quad (5)$$

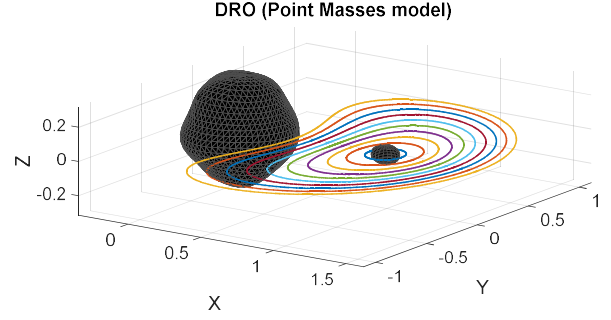


Fig. 3. Representation of DRO family in the point masses binary system. Real shape of asteroids has been introduced to give a better understanding of orbits dimensions.

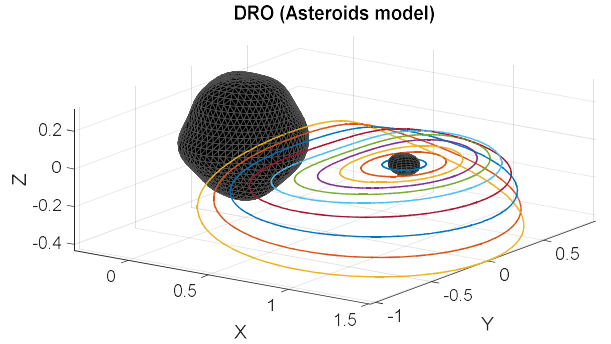


Fig. 4. Representation of DRO family in the asteroids binary system. The gravitational field is coherent with the real shape of the objects.

All possible combinations among the orbits database are generated and evaluated according to the value given by Eq. (5). An initial screening removes solutions involving proximity flight, hence all couples with orbits belonging to the same equilibrium points of the binary system. The remaining couples are mapped in terms of the cost value, and a best couple for each orbit family combination is identified and saved (see Fig. 5 and 6). A last step in the selection process is introduced through the generation of a 3D Pareto front, where axes correspond to the single objectives from Eq. (1), (2) and (4) (shown in Fig. 7), and non-dominant solutions can be discarded.⁶

The main drawback related with the direct exploitation of the combined couples is the non-multiplicity (within reasonable times) of the periods of the two orbits forming the couple: the values of the objective costs will be true for the first period of the orbit with longest duration, then a shifting phase causes the loss of the initial configuration until it is restored again after a certain time (which could be very large). The local optimization process allows to restore periodicity in the formation, while trying to reduce to minimal values the costs of the function.

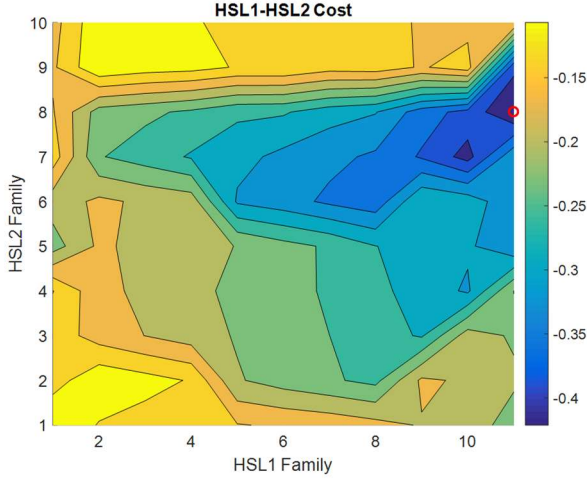


Fig. 5. Overall cost map for couples of families HSL1 and HSL2. Axes represent the numbering of orbits in each family, from the smallest to the widest. The red circle identifies the combination of the two families with the lowest cost.

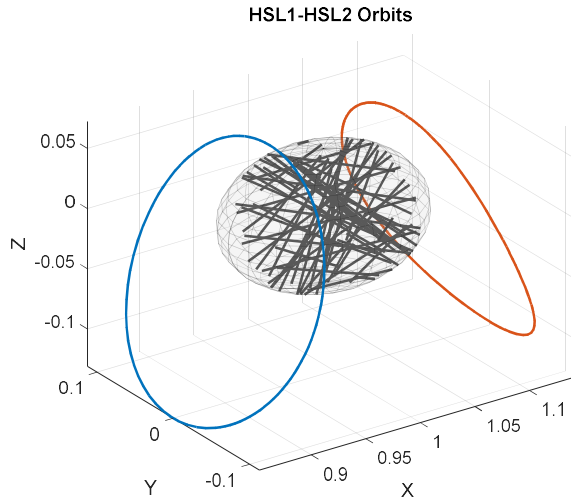


Fig. 6. Representation of HSL1-HSL2 best configuration. Grey lines inside Didymoon represent the mapping directions during the natural orbital motion of the two spacecraft.

Thanks to the scalar nature of the overall cost function, the classical optimization scheme based on Lagrange multipliers can be exploited,

$$\begin{cases} J_c = J - \int_0^T (\underline{\lambda}^T \underline{g}) dt \\ \delta J_c = 0 \end{cases} \quad (5)$$

from which a boundary value problem, composed by a set of 24 first order ODE and relative boundary conditions (the continuity between initial and final state, to ensure periodicity), is obtained.⁷⁾

$$\begin{cases} \dot{\underline{\eta}} = \underline{f}(\underline{\eta}) \\ \underline{\eta}(T) - \underline{\eta}(0) = \underline{0} \end{cases} \quad (6)$$

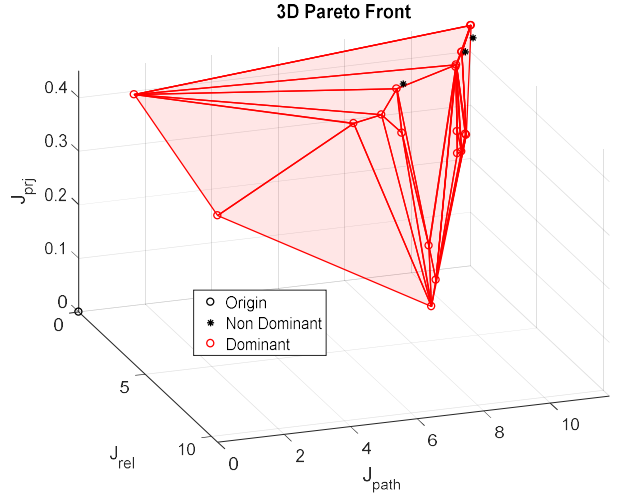


Fig. 7. Pareto front of the best configurations group. Red surface connects all the dominant solution, while black dots represent the non-dominant couples.

The system accounts for the satisfaction of the objectives, while keeping the dynamics coherent with the MCR3BP (with the real shape of the attractors), however, in the current form, it is not capable of detecting collision trajectories with the attractors. To work around the problem, the set of equations is augmented with 4 inequality constraints (2 per satellite), stating the violation of the non-collision condition. For each satellite, the 2 constraints read:

$$\begin{cases} \frac{1}{R} \left((x_j + \mu)^2 + (y_j)^2 + (z_j)^2 \right) - 1 > 0 \\ \left(\frac{x_j + \mu - 1}{a} \right)^2 + \left(\frac{y_j}{b} \right)^2 + \left(\frac{z_j}{c} \right)^2 - 1 > 0 \end{cases} \quad (7)$$

Eq. 7 states that satellite number “j” shall have a norm of the distance from main attractor higher than the maximum radius of the asteroid, and a norm of the distance from secondary attractor outside the surface of the ellipsoid. If at least one of the 4 inequalities is not satisfied, it is converted into an equality relationship (to be included in the system of Eq. 6).

$$\underline{c}(\underline{\eta}) = \underline{0} \quad (8)$$

Letting the formation period free to vary, the solution of the system composed by Eq. 6 and 8 will keep the periodicity property, while moving outside the initial search space. The obtained DAE system is characterized by discontinuities introduced by collision constraints, therefore techniques like multiple shooting are particularly suitable for this purpose.

In the specific problem under study, the Newton method (which is preferred due to its high rate of convergence) causes overshooting problems and consequent failures in finding the optimized solutions, therefore a Levenberg-Marquardt scheme is used.⁸⁾ Along the guess orbits, discrete nodes are generated and their state is saved and compared with the one propagated from the previous node: the difference of the two state values represents the objective function to be nulled. Together with all the nodes connections, boundary conditions and “active” non-collision constraints (referred only to colliding nodes) are added to the set.

$$\underline{F} = \begin{bmatrix} (\underline{p} - \underline{p}_n)_j \\ (\underline{N} - \underline{N}_1)_j \\ (\underline{c}(\underline{p}))_k \end{bmatrix}, \quad j = 1:N, \quad k = 1:N_c \quad (9)$$

For each iteration “ i ”, the update in the state of the nodes reads:

$$\underline{X}_{i+1} = \underline{X}_i - \left(\underline{J}_M^T \underline{J}_M + \lambda_r \text{Diag} \left(\underline{J}_M^T \underline{J}_M \right) \right)^{-1} \underline{J}_M^T \underline{F}_i \quad (10)$$

and the residual to be brought to zero is evaluated as:

$$r = \frac{1}{2} \underline{F}^T \underline{F} \quad (11)$$

The damping parameter λ_r is updated at each iteration according to the new value of the residual with respect to the previous one.

The dimensions of the problem will be variable due to the activation and deactivation of collision constraints: when a node falls into asteroids surface, a row presenting the constraint of Eq. 8 is added, and remains in the system until the non-collision condition is satisfied again.

The reduced convergence rate of the LM algorithm is partially restored through some modifications in the method. In particular, the “uphill” and the “delayed gratification” techniques,⁹⁾ are introduced. The first relaxes the comparison of the new residual with the old one, allowing local increment if the following conditions are satisfied:

$$\begin{cases} d\underline{X}_i = \underline{X}_{i+1} - \underline{X}_i \\ \beta_i = \frac{d\underline{X}_i \cdot d\underline{X}_{i-1}}{\|d\underline{X}_i\| \|d\underline{X}_{i-1}\|} \\ (1 - \beta_i)r_i < r_j, \quad j = 1:i-1 \end{cases} \quad (12)$$

The approach allows to move faster in zones of the function where “canyon-like” shapes are present, and to avoid the algorithm to get stuck. In the present work, the term $(1-\beta)$ is evaluated under square root, to make the procedure more robust and avoid convergence failures

The second technique focuses on the update of parameter λ :

- If Eq. 12 is satisfied, λ is decreased of a quantity “a”
- If Eq. 12 is not satisfied, λ is increased of a quantity “b” such that $b < a$

The difference on the increasing/decreasing step reduces the overall number of jumps on λ values, potentially speeding up the convergence rate near the solution.

3. Results

This section presents the most significant results of the optimization, through a comparison with the initial guesses and an analysis of the possible reasons behind the phenomena observed in the overall process.

The complete set of orbit families considered is composed by:

- Lyapunov families (around L1 and L2)
- Northern and southern Halo families (around L1 and L2)
- DRO family (around Didymoon)
- SPO family (around L4)

The preliminary combinatorial process and dominance search lead to the definition of 20 sub-optimal couples, characterized by a significant variety in the single objectives satisfaction: consequently, a specific couple may show a low overall cost through a single objective minimization, while keeping the other contributions nearly unchanged or even worsened. This effect can be observed directly from the Pareto front displayed in Fig. 7. The advantage of this behavior resides in the different choices available, depending on the user’s preferences.

The optimization causes, as first effect, a uniformation of the single objectives toward a common mean value (in most cases), with consequent reduction/increment of the overall cost and the creation of a more balanced and less diversified set, which becomes more interesting if all the objectives need to be satisfied at the same time. Among the optimized solutions, 3 results groups could be identified:

- 3 “Failed” solutions, where the algorithm failed to converge or got stuck during the process.
- 10 “Trivial” solutions, representing physically valid solutions, but related to configurations known a priori (spacecraft located at equilibrium points).
- 7 “Good” solutions, where physically coherent and non-trivial configurations are found.

With the only exception of failed solutions, the distribution of the configurations in the space of the objectives defines the new Pareto front, as shown in Fig. 8.

From the comparison with Fig. 7, it is observed a conservation of the planar shape of the front. Most initial configurations fall into the upper left region, where best relative motion values and worst mapping and path length properties are present: here lie all the solutions involving the equilibrium points, that is the “trivial” group. The superposition of many configurations in the same region causes also the generation of many non-dominant solutions.

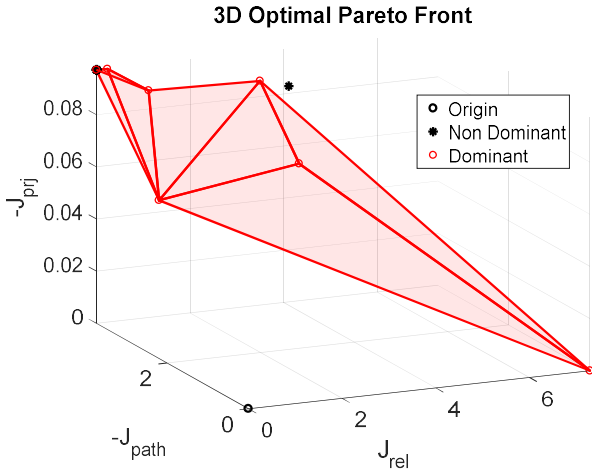


Fig. 8. Pareto front for the set of optimal configurations.

The cause of the accumulation of solutions in the neighborhood of the trivial region may reside in the flat shape of the Pareto front: the absence of a marked convexity in the front's shape generates difficulties in the search of scattered solutions through weighted sum scalarization methods.¹⁰⁾ To improve the number and the variety of acceptable solutions, further improvements in the local search method shall be introduced.

In the next paragraphs, the three most meaningful solutions from the “good” set are analyzed, represented by DRO-HSL2, HNL1-DRO and HSL1-DRO.

3.1. DRO-HSL2

The optimization of DRO-HSL2 leads to a decrement of the overall cost, with improvements in relative motion reduction and mapping maximization, at the cost of lower lengths (see Table 1).

Table 1. Objectives and overall costs for DRO-HSL2 guess and optimized configurations.

	J_{rel}	J_{path}	J_{prj}	J
Guess	1.1685	-0.7371	-0.0422	0.3892
Optimal	0.7661	-0.6564	-0.0460	0.0637

Trajectories appear closer to each other and to Didymoon's surface. The smallest dimensions and the vicinity to the attractor allow longer mapping times, lower relative oscillations and a lower formation period. The visual representation of the orbits before and after the optimization is provided in Fig. 9 and 10.

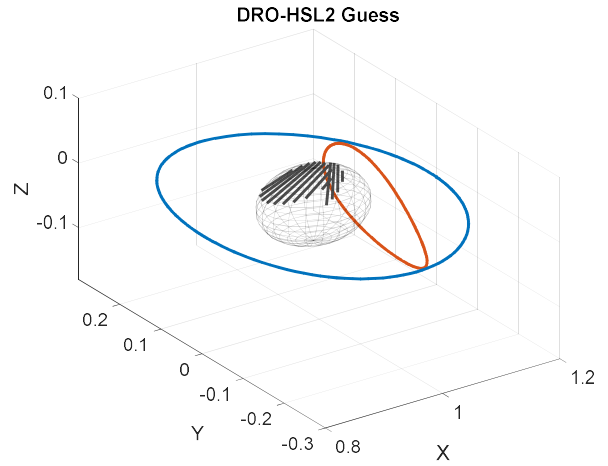


Fig. 9. Guess configuration for DRO-HSL2 couple.

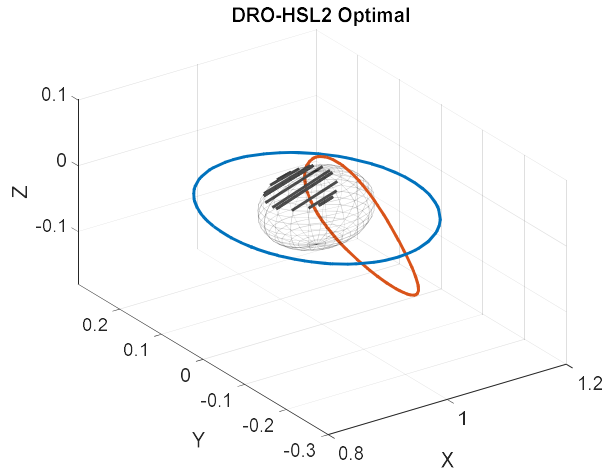


Fig. 10. Optimal configuration for DRO-HSL2 couple.

It is observed that the modification of the orbits maintained their original shape and out-of-plane properties, fact that can be attributed to the quasi-periodicity of the initial guess (see Fig. 11): without the need of relevant modifications to find perfect periodicity, the optimization becomes more effective on the cost reduction task.

Furthermore, the activation of non-collision constraints prevents the orbits from shrinking too much and losing mapping and path properties.

A final observation regards the mapping of the asteroid: while the covered surface in the optimal configuration appears lower than the one of the guess, in the former case a second passage above the same area (within the formation period) is measured, therefore the effect on the objective is doubled. To make the algorithm distinguish passages on the same areas, the objective expression shall be further modified.

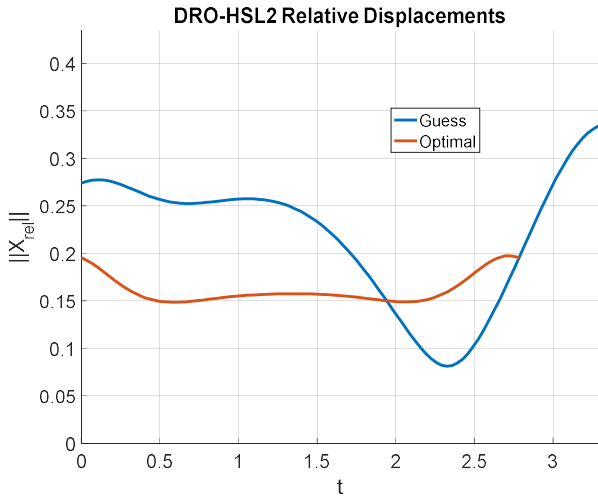


Fig. 11. Relative distance between spacecraft for the guess and optimal configuration of DRO-HSL2 couple. The guess configuration show a very small shift between initial and final displacement (quasi-periodicity). The optimized solution is characterized by a nearly constant distance and a shorter period.

3.2. HNL1-DRO

The optimization process causes, in contrast with the previous solution, an overall increment of the total cost (see Table 2).

Table 2. Objectives and overall costs for HNL1-DRO guess and optimized configurations.

	J_{rel}	J_{path}	J_{prj}	J
Guess	4.7298	-4.7780	-0.0332	-0.0814
Optimal	2.8912	-1.6515	-0.0272	1.2126

Significant modifications of the single objectives are measured: the halved value of the optimal relative displacement is counterbalanced by an even greater reduction of the trajectories path and a small reduction of mapping area, thus making the overall cost grow up.

As a result, the optimized orbits are shrunk and modified towards planarity (in the Didymain-Didymoon orbital plane), so that Halo orbit is transformed to a Lyapunov. The comparison between the configurations is depicted in Fig. 12 and 13.

The out-of-plane component is not conserved during the optimization, despite the presence of the mapping, highlighting another drawback of this contribution: the mathematical expression adopted does not distinguish the in-plane component from the out-of-plane component (which may be fundamental in terms of scientific return), thus requiring future improvements for this purpose.

Figure 14 shows the trend of relative displacements and the effects of the optimization process.

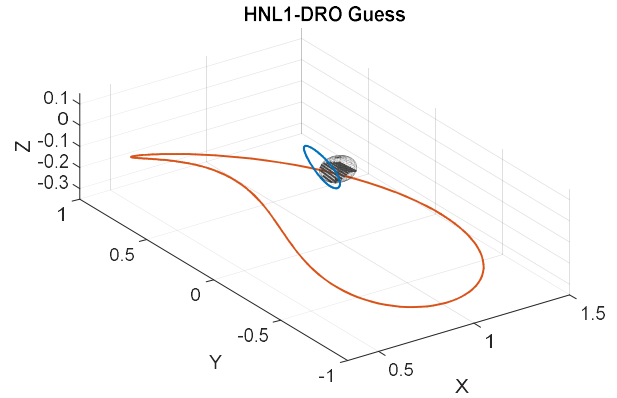


Fig. 12. Guess configuration for HNL1-DRO couple.

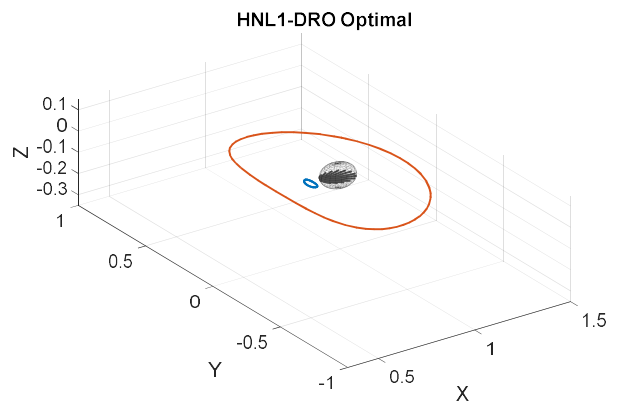


Fig. 13. Optimal configuration for HNL1-DRO couple.

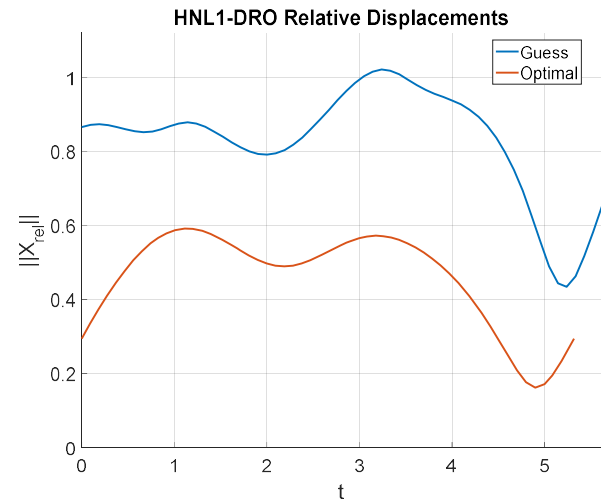


Fig. 14. Relative distance between spacecraft for the guess and optimal configuration of HNL1-DRO couple. The guess configuration shows a significant shift between initial and final displacement. The optimized solution is characterized by lower (but still present) displacements and a slightly shorter period.

The increment of the overall cost may be related to the marked non-periodicity of the guess couple: the process is forced to ensure connection between initial and final state, thus making the cost change (possibly towards higher values) before

the real optimization begins, and affecting negatively the final (optimal) value.

3.3. HSL1-DRO

The couple HSL1-DRO shows tendentially opposite behaviors with respect to other solutions. As in the previous cases, an initial non-periodicity leads to higher overall costs in the optimized solution, however, the trend of the single objectives is inverted: an improvement on the mapping is counterbalanced by worse values in terms of both path length and relative motion, as shown in Table 3.

Table 3. Objectives and overall costs for HSL1-DRO guess and optimized configurations.

	J_{rel}	J_{path}	J_{prj}	J
Guess	6.7063	-3.8927	-0.0899	2.7237
Optimal	7.2949	-3.7274	-0.0972	3.4703

The path and relative motion worsening are explained looking at the geometrical modifications that the algorithms applies to the orbits. From the comparison between the couple before and after the optimization process (see Fig. 15 and 16), it is noticed that Halo orbit is shrunk in the direction of its equilibrium point (coherently with the other configurations), while the DRO is enlarged (with increments both in dimensions and period). Consequently, although the final overall path results slightly lower (due to the HSL1 shrinkage, which nulls the effect from the larger DRO), the augmented distance between orbits makes relative oscillations more relevant (as shown in Fig. 17).

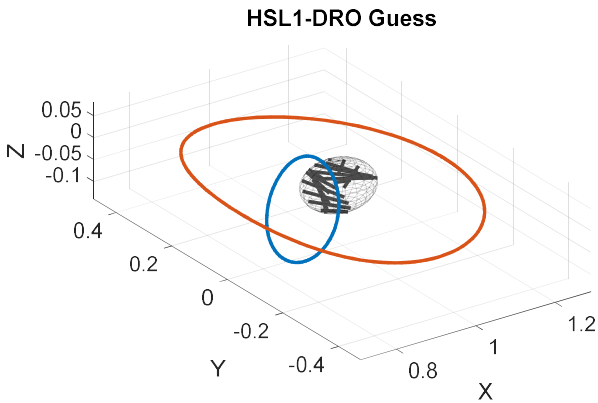


Fig. 15. Guess configuration for HSL1-DRO couple.

The resulting configuration is again characterized by planar trajectories, and the mapping of the asteroid will be limited to Dydimoon’s equatorial disc.

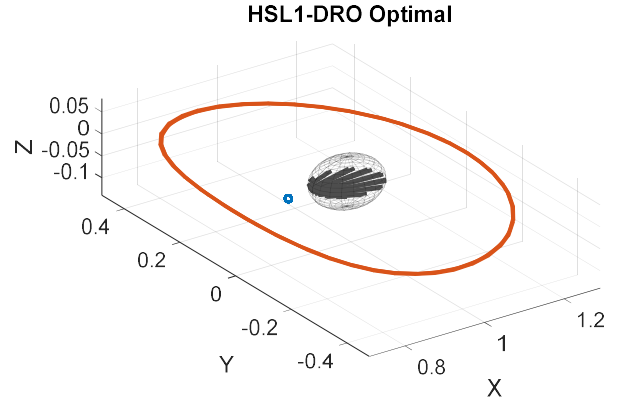


Fig. 16. Optimal configuration for HSL1-DRO couple.

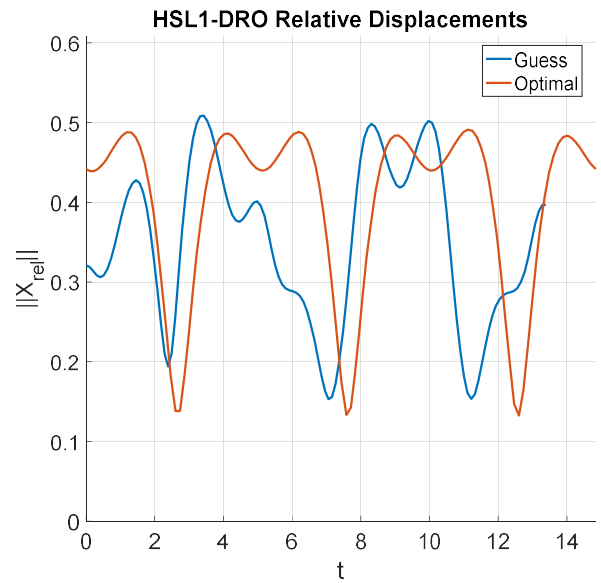


Fig. 17. Relative distance between spacecraft for the guess and optimal configuration of HSL1-DRO couple. Differently from the other configurations, the optimal solution is characterized by higher displacements and a longer period.

4. Conclusions

The application of an optimization algorithm based on combinatorial process of already known, discrete solutions, and a subsequent local optimization through analytical expressions, demonstrated to be a suitable approach to deal with chaotic and complex problems as the one faced in this paper. The strategy, although derived from simple and basic optimization processes, was capable of dealing with a multiple objective, complex problem, providing a set of suitable solutions for a two-nanosatellite formation, and laid the foundations for many improvements in various aspects faced in the development of the algorithm.

Besides that, few drawbacks have been encountered in the application of this strategy, in terms of mission objectives and optimization behaviors. From them, new directions for the development of the present project could be identified.

Together with a review of the already defined mission

objectives, and their extension to more complete expressions (in particular for the mapping contribution), the cost function shall be augmented with more objectives, to be added or removed selectively by the user, to best adapt to various mission designs: particularly of interest are constraints on orbital stability and propellant costs for maneuvers (to reach the formation configuration).

Secondly, enhancements on the algorithm shall be introduced, in terms of:

- Dynamics propagation: selective reduction of polyhedron's faces (Didymain model) to speed up the integration without affecting the precision of the trajectory.
- Algebraic constraint management: restatement of the introduction of algebraic constraints to avoid blockings in the algorithm when large orbit segments fall into asteroids' surface.
- Multiple objectives scalarization: improvements in the management of objectives, to avoid accumulation points (caused by low convexity of the Pareto frontier) and favor higher spreading of the solutions in the objectives' space.

Finally, for a more realistic representation of binary systems, extension to elliptical three-body problem, and the introduction of independent rotations of the attractors, together with external

perturbation sources, will be included in the analysis.

References

- 1) Ferrari, F.: Formation flying dynamics in circular restricted three body problem and applications to binary asteroid systems, (2013).
- 2) Colagrossi, A.: Coupled dynamics around irregularly shaped bodies with enhanced gravity field modelling, (2015).
- 3) Werner, R. A. and Scheeres, D. J.: Exterior gravitation of a polyhedron derived and compared with harmonic and mascon gravitation representations of asteroid 4769 Castalia, *Celestial Mechanics and Dynamical Astronomy* 65.3 (1996), pp. 313-344.
- 4) MacMillan, W. D.: The theory of the potential, (1958).
- 5) Capannolo, A., Lavagna, M., Ferrari, F. and Lunghi, P.: Nanosatellite Formation Flying to Enhance Science in Binary Asteroid Environment, *6th International Astronautical Congress (IAC)*, Guadalajara, Mexico, 26-30 September 2016.
- 6) Grodzevich, O., and Oleksandr, R.: Normalization and other topics in multi-objective optimization, 2006.
- 7) Gill, P. E., Murray, W. and Wright, M. H.: Practical optimization, (1981).
- 8) Bates, D. M. and Watts, D. G.: Nonlinear regression analysis and its applications, Wiley, (1988).
- 9) Transtrum, M. K. and Sethna, J. P.: Improvements to the Levenberg-Marquardt algorithm for nonlinear least-squares minimization, *arXiv preprint arXiv:1201.5885* (2012).
- 10) Caramia, M., and Dell'Olmo, P.: Multi-objective management in freight logistics: Increasing capacity, service level and safety with optimization algorithms, Springer Science & Business Media, (2008).